Overpotential-Controlled Nucleation of Ni Island Arrays on Reconstructed Au(111) Electrode Surfaces

F. A. Möller, O. M. Magnussen, and R. J. Behm
Abteilung Oberflächenchemie und Katalyse, Universität Ulm, D-89069 Ulm, Germany
(Received 24 June 1996)

In situ scanning tunneling microscopy observations on Ni electrodeposition on reconstructed Au(111) electrodes are presented, which reveal that Ni nucleation proceeds in three distinct, potential-dependent steps: place exchange of Ni with Au atoms at the elbows of the herringbone reconstruction (overpotential $\eta \geq 0$ mV), nucleation of Ni islands on top of these substitutional Ni atoms ($\eta \geq 80$ mV), and nucleation at the step edges of the Au substrate ($\eta \geq 100$ mV). This allows one to selectively control the growth via the potential and, in particular, to create nanostructures composed of regularly spaced Ni islands. [S0031-9007(96)01900-X]

PACS numbers: 68.55.–a, 61.16.Ch, 81.15.Pq

The spontaneous formation of nanostructures by epitaxial growth of submonolayer films has raised considerable interest [1–10]. A prominent example is metal deposition on reconstructed Au(111), where regular arrays of admetal islands can be formed by preferential nucleation at uniformly spaced dislocation sites of the reconstructed Au surface layer. As revealed by scanning tunneling microscopy (STM) studies in ultrahigh vacuum (UHV), Ni [4–7], Co [8,9] , and Fe [5,10] exhibit this nucleation behavior, while for other metals this preferential nucleation was not observed [5,6,11]. In contrast to these studies of deposition under UHV conditions the assembly of similar nanostructures by electrochemical methods has not yet been reported. Here we present *in situ* STM observations of the Ni electrodeposition on reconstructed Au(111) electrodes which demonstrate that depending on the overpotential $\eta = U - U_{\mathrm{Me/Me}^{z+}}$ ($U_{\mathrm{Me/Me}^{z+}}$ is the corresponding Nernst potential) distinctly different nucleation behavior occurs: (a) place exchange with Au atoms at the dislocation sites of the reconstructed Au surface, (b) growth of Ni islands *on top* of the substitutional Ni, and (c) nucleation of Ni islands at step edges. In particular, (a) and (b) lead to the selective nucleation at regularly arranged sites on the Au surface in a narrow potential regime, allowing the formation of similar nanostructures as obtained under UHV conditions. The activation of qualitatively different nucleation and growth mechanisms with increasing overpotential, a phenomenon proposed long ago to explain electrochemical measurements [12], can be rationalized by an energetic preference for the place exchange and different kinetic barriers for the nucleation at the various *on top* sites. Finally, the *in situ* observation of these distinct nucleation steps allows one to unanimously assign preferential place exchange as the physical origin for preferential nucleation at the dislocation sites, as was recently proposed based on UHV-STM observations of very low Ni coverages on Au(111) and on thermodynamic considerations [7].

A detailed description of the home-built electrochemical STM used in the experiments and of the experimental procedures is given in Refs. [13,14]. Experiments were performed in modified Watts electrolyte ($10^{-2}M\,H_3BO_3$, $10^{-4}M$ HCl, and $10^{-3}M\,NiSO_4$) prepared from suprapure H_3BO_3 and HCl, p.a. grade $NiSO_4$, and Milli-Q water. At the beginning of each experiment the Au sample was freshly prepared by flame annealing [15] and then immersed into the electrolyte at -0.2 V. The potentials of sample and tip were controlled potentiostatically versus an Ag/AgCl (KCl sat.) reference electrode with the tip potential usually kept 50–100 mV below the sample potential. STM images were obtained in constant current mode with tunneling currents between 1 and 10 nA and are presented as top view images with lighter colors corresponding to higher surface areas.

Prior to the STM measurements, cyclic current-voltage curves (voltammograms) of Au(111) in the modified Watts electrolyte were recorded in a separate electrochemical cell. The onset of nickel deposition manifests itself as a broad shoulder on the large negative current caused by hydrogen evolution and hence Ni deposition cannot be assessed from the negative potential sweep. Instead, the amount of Ni deposition was estimated by maintaining a fixed deposition potential for up to 15 min and then measuring the charge in the Ni dissolution peak, which is shifted to -0.2 V, well above the range of hydrogen evolution. According to these stripping experiments, measurable Ni deposition starts at about -0.60 V, i.e., well below the Ni/Ni^{2+} Nernst potential (-0.52 V). In particular, no underpotential deposition (UPD) is observed for Ni on Au(111). This is in agreement with previous electrochemical and quartz microbalance studies on polycrystalline Au, which also found large overpotentials for Ni deposition [16,17]. The overpotential is rather independent of the electrolyte composition with experiments in pure Ni sulfate or Ni nitrate solution resulting in only slightly higher overpotentials [18]. The anodic shift of the Ni dissolution peak has been attributed to stabilization of the deposit by coadsorbed (or absorbed) hydrogen [19]. In subsequent potential sweeps the cyclic voltammogram is completely reproducible, suggesting that the deposited Ni does not alter the Au(111) surface significantly.

In contrast to the results of the electrochemical measurements, the *in situ* STM experiments demonstrate Ni-induced structural changes in the Au(111) substrate at potential well above -0.6 V. This phenomenon is demonstrated in the two successively recorded STM images presented in Fig. 1. Figure 1(a) shows an atomically flat terrace of the well prepared Au(111) substrate surface at -0.2 V. The surface exhibits a long-range modulation pattern of double rows, which is characteristic for the Au(111) reconstruction and which has been reported in previous UHV [4,20,21] and electrochemical [22,23] STM studies. In Fig. 1(a) these double rows form a periodic zigzag (or herringbone) structure with an even larger unit cell, which indicates a very well prepared surface [4,21]. By immersing freshly annealed samples under potential control at potentials ≤ 0 V the ordered zigzag pattern could be reproducibly prepared on the Au(111) surface. A more random arrangement of reconstruction domains resulted if the reconstruction was lifted and electrochemically formed again by cycling the potential to values above 0.15 V, in agreement with previous results [23,24]. The reconstruction was found on Au(111) surface areas free of Ni deposits in the entire potential range studied (-0.7 to 0.15 V). It is particularly important to note that the turns of the reconstruction stripes ("elbows") in Fig. 1(a) are completely free of defects.

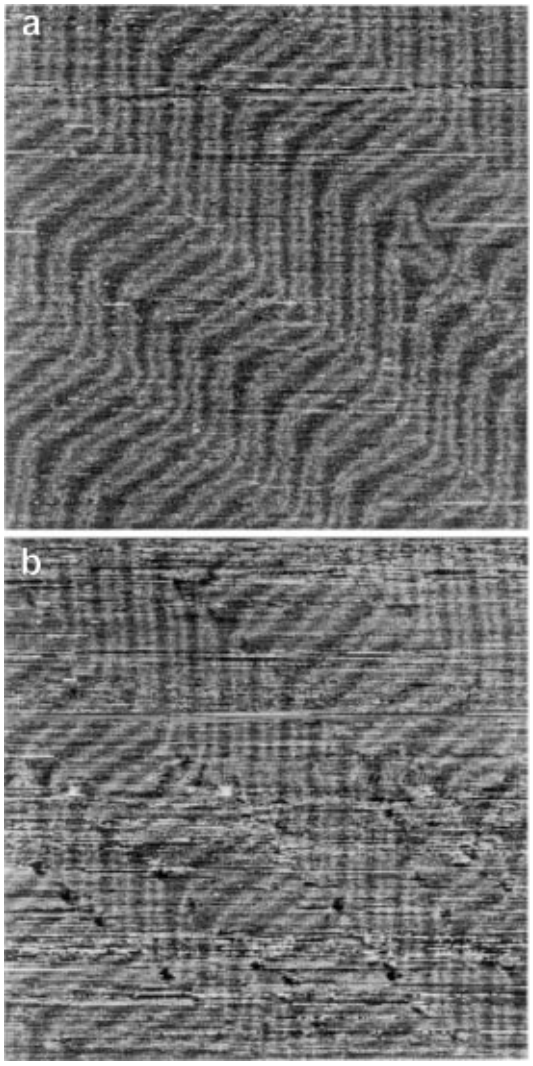

FIG. 1. Two successively recorded STM images of Au(111) in modified Watts electrolyte showing (a) the reconstructed surface at -0.2 V and (b) the formation of holes at the elbows of the herringbone reconstruction after a potential change to -0.6 V (900×900 Å^2).

In the following we show the structural changes during Ni deposition. At the beginning of Fig. 1(b) (upper edge) the potential was decreased to -0.6 V. Apart from a reduced stability of the STM tip due to hydrogen evolution the topography of the reconstructed surface essentially seems to be the same as in Fig. 1(a). On a closer look, however, changes are observed in the lower half of the image at the elbows of the reconstruction, which are now decorated by small holes of approximately 20 Å in diameter. These holes are only 0.5 Å deep, which even if finite size effects are taken into account is much shallower than monatomic deep pits in the Au substrate. According to other STM series these "holes" are rapidly formed at a well-defined potential, which is within 10 mV of the Ni/Ni^{2+} Nernst potential of -0.52 V, and can be seen from there down to -0.7 V (the most negative potential where the "bare" Au(111) surface could be observed) without noticeable changes in size. Raising the potential back to -0.3 V, where according to the voltammogram Ni dissolution commences, the holes slowly disappear, leaving an undistorted reconstructed Au surface behind, similar to the one in Fig. 1(a). Since the holes are only observed in the presence of Ni in the electrolyte, they are interpreted as Ni atoms which have substituted Au surface atoms via place exchange (see below). A detailed analysis shows that the holes are situated at the bulged elbows of the reconstruction lines denoted by "type-x" in Ref. [4], i.e., exactly at the position where the two-dimensional lattice of the reconstructed Au surface layer exhibits dislocations [4]. Also, the size of the holes is in good agreement with the size of the distortion zone around the dislocations as estimated from UHV observations [4–6].

The substitution of Au atoms by Ni at the elbow sites has important consequences for the nucleation behavior. This is shown in the series of STM images in Fig. 2, recorded in another experiment. All three images were obtained in approximately the same surface area of an atomically flat terrace, with a Au step edge in the upper right corner of Figs. 2(a) and 2(b) [the image in Fig. 2(c) is shifted by $\approx$500 Å to the left, as a reference the same island is marked by an arrow in Figs. 2(b) and 2(c)]. In Fig. 2(a), which was recorded directly after decreasing the potential to -0.6 V, the surface topography largely resembles that in Fig. 1(b), with holes at almost every elbow of the Au reconstruction. After keeping the potential for several minutes at -0.6 V, nucleation of the first Ni *adlayer* islands is detected [Fig. 2(b)]. No formation of Ni islands was observed at more positive potentials. This indicates

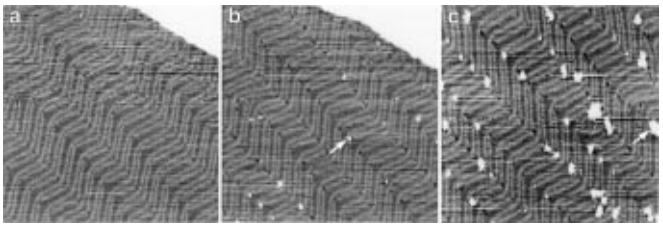

FIG. 2. Series of STM images recorded on Au(111) in modified Watts electrolyte (a) directly after a potential change from -0.2 to -0.6 V, (b) 3 min at -0.6 V, and (c) 20 min at -0.6 V showing slow nucleation of Ni islands *on top* of the holes (1050×1050 Å^2); the image in (c) is shifted with respect to (a) and (b) by $\approx$500 Å along the x direction [arrows mark the same island in (b) and (c)].

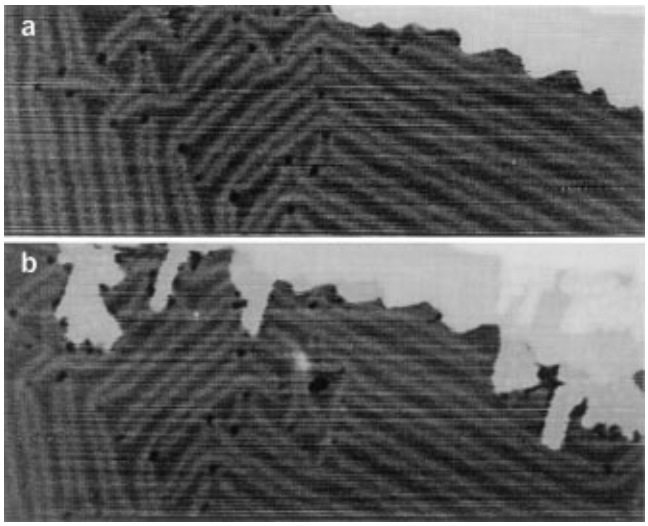

FIG. 3. STM images of Au(111) in modified Watts electrolyte close to a step edge at (a) -0.59 V (1150×450 Å^2) and (b) after keeping the potential for 3 min at -0.63 V (1150×550 Å^2) showing nucleation of Ni islands at step edges.

that Ni *adlayer* nucleation requires an overpotential η of 80 mV, in good agreement with the electrochemical results. At -0.6 V nucleation proceeds exclusively at the holes which were previously formed at the elbows (i.e., *on top* of substitutional Ni atoms). The island height of 1.7 Å is slightly less than the 1.9 Å expected for Ni atoms in Au(111) hollow sites in a hard sphere model, most likely due to electronic effects; the island diameters range between 5 and 30 Å. On a freshly annealed Au surface the elbows and consequently the holes, which provide the nucleation sites, are regularly arranged so that the islands start to form an ordered pattern. This can be seen in Fig. 2(c), recorded after a waiting period of 23 min at the same potential. After this time Ni islands have nucleated at about 50% of the elbows of the Au reconstruction corresponding to an island density of about 10^{12} cm^{-2}. The coverage, however, is less than 0.1 monolayer, hence the growth rate is very low. A very small fraction of the Ni islands (at this potential $\approx$2%) is not located at the elbows but forms at arbitrary sites on the Au(111) surface (probably due to contamination effects). The resulting topography strongly resembles that observed for UHV deposited Ni on Au(111) [4–7] with most of the islands arranged along regularly spaced chains with interisland distances in the $[1\bar{2}1]$ direction of about 73 Å and a spacing between neighboring chains of 140 Å. No nucleation at step edges is observed at -0.6 V, even after an observation time of more than an hour. Hence, the elbows are the preferential nucleation sites at this potential.

At about 20 mV higher overpotentials, i.e., at $\eta =$ 100 mV, the nucleation and growth behavior changes considerably, as exemplified by the STM images in Fig. 3. As in the previously described experiment, the initial Au(111) surface (not shown) had been completely reconstructed, albeit not as well ordered as in Fig. 2(a) due to a preceding potential cycle. Directly after decreasing the potential to -0.6 V [Fig. 3(a)] holes are visible at the elbows and U-shaped endings, which contain similar dislocations [21], but no Ni deposit in the form of *adlayer* islands or at step edges is found. In contrast, 3 min after a further change to -0.63 V [Fig. 3(b)] Ni deposition at the lower terrace side of steps of the Au(111) substrate is observed. The Ni deposit, which can be easily distinguished from the Au step due to its different height, does not wet the Au step edge. Instead the nuclei grow as isolated, anisotropically shaped islands into the Au terrace (a detailed description of structure and growth of the Ni film under these conditions will be given elsewhere [18]). Island nucleation at the elbows *on top* of the holes proceeds with roughly the same rate as at -0.6 V. Since this is much lower than the rate of nucleation at Au step edges the latter mechanism becomes dominant at overpotentials of 100 mV.

The observed sequence of distinctly different nucleation processes at increasing overpotentials (Ni exchange, adisland nucleation at elbows, adisland nucleation at step edges) can be understood in a simple picture. First, the difference in potential for deposition of *adlayer* islands *on top* the surface and for deposition via place exchange is considered. Deposition via place exchange is only possible if substitutional Ni is thermodynamically stable and if the kinetic barrier for the exchange process is sufficiently low at room temperature. Apparently one or both of these conditions are fulfilled only at the dislocation sites within the Au layer. The low kinetic barrier can qualitatively be explained by the specific coordination of Au surface atoms in the center of the elbows (see Refs. [4,21]), which favors exchange at these sites. Likewise, because of the higher surface free energy of Ni than that of Au, incorporation of Ni into the Au surface layer will reduce the total free energy of the system with respect to that of *on top* Ni. In addition, the exchange of Au with the smaller Ni atoms may help to reduce the inherent stress at these dislocation sites. Consequently, the equilibrium potential for deposition via place exchange should be more positive than that of *on*

top deposition. This is similar to underpotential deposition, where an increase in the binding energy between ad- and substrate metal (relative to the admetal-admetal bond) causes a positive shift of the equilibrium potential of the first monolayer, except for that in the present case only the elbow sites are energetically favored. On the other hand, the stronger Ni-Ni bond as compared to Ni-Au [25] should shift the onset of Ni deposition *on top* of Au surfaces for thermodynamic reasons to potentials negative of the Nernst potential, in good agreement with the experimentally observed overpotential of 80–100 mV for Ni *adlayer* deposition.

The different overpotentials required for nucleation of Ni *adlayer* islands at different sites (*on top* of substitutional Ni or at Au step edges) can be rationalized by kinetic nucleation theory. Following that, a certain overpotential is required to attain supersaturation. Considering the stronger Ni-Ni interactions as compared to the Ni-Au interactions, it is straightforward that nucleation preferentially takes place *on top* of substitutional Ni rather than on the pure Au terraces, since Ni adatoms have a longer lifetime on these sites because of the additional stabilization ("heterogeneous nucleation").

Finally, an even higher kinetic barrier of $\eta = 100$ mV is required for nucleation at step edges. At these sites some stabilization may be provided by the Au edge atoms, but obviously this is less than the stabilization by substitutional Ni atoms at the elbow sites. This also implies that nucleation in the midst of the Au terraces, without any additional stabilization, would require an even larger overpotential. Correspondingly, the latter was not observed experimentally at $\eta \leq 100$ mV. A lower boundary for the nucleation of Ni on a defect-free, hexagonally ordered Au surface is provided by STM experiments of Ni deposition on reconstructed Au(100), where an overpotential of $\eta = 150$ mV was required to initiate nucleation in the midst of extended domains of the "hex" reconstruction [18].

Our results and interpretation agree perfectly with the nucleation mechanism proposed for Ni/Au(111) in a recent UHV-STM study [7], where the authors concluded from observations at very low coverage that nucleation of Ni adlayer islands at the elbow sites is preceded and caused by Ni exchange at these sites. Interestingly, in another UHV study [6] it was observed that in the absence of elbow sites, on a large terrace with only one reconstruction domain, nucleation exclusively occurred at step edges, confirming our picture that nucleation in the midst of flat terraces (without elbow sites) is least likely to occur.

In summary, we have shown that Ni deposition on Au(111) proceeds in three different nucleation steps, which require different overpotentials and hence can be controlled by the deposition potential. Our results indicate a nucleation mechanism involving place exchange of Ni at well-defined surface dislocations ("elbows"), subsequent adlayer nucleation *on top* of substitutional Ni, and finally nucleation at Au steps. This allows the potential-controlled selection between different nucleation and growth mechanism and, in particular, within a narrow potential regime the formation of nanostructures via the selective nucleation at certain, regularly spaced positions of the Au substrate. More general, this demonstrates the possibility to generate such two-dimensional nanostructures in the electrochemical environment and to control their growth via the deposition potential.

[1] C. Günther, S. Günther, E. Kopatzki, R. Q. Hwang, J. Schröder, J. Vrijmoeth, and R. J. Behm, Ber. Bunsen-Ges. Phys. Chem. **97**, 522 (1993).

[2] H. Röder, E. Hahn, H. Brune, J.-P. Bucher, and K. Kern, Nature (London) **366**, 141 (1993).

[3] K. Bromann, H. Brune, H. Röder, and K. Kern, Phys. Rev. Lett. **75**, 677 (1995).

[4] D. D. Chambliss, R. J. Wilson, and S. Chiang, Phys. Rev. Lett. **66**, 1721 (1991).

[5] D. D. Chambliss, S. Chiang, and R. J. Wilson, Mater. Res. Soc. Symp. Proc. **229**, 15 (1991).

[6] D. D. Chambliss, R. J. Wilson, and S. Chiang, J. Vac. Sci. Technol. B **9**, 933 (1991).

[7] J. A. Meyer, I. D. Baikie, E. Kopatzki, and R. J. Behm, Surf. Sci. (to be published).

[8] B. Voigtländer, G. Meyer, and N. M. Amer, Phys. Rev. B **44**, 10 354 (1991).

[9] J. Wollschläger and N. M. Amer, Surf. Sci. **277**, 1 (1992).

[10] J. A. Stroscio, D. T. Pierce, R. A. Dragoset, and P. N. First, J. Vac. Sci. Technol. A **10**, 1981 (1992).

[11] C. A. Lang, M. M. Dovek, J. Nogami, and C. F. Quate, Surf. Sci. **224**, L947 (1989).

[12] R. Kaischew and B. Mutaftschiev, Electrochim. Acta **10**, 643 (1965).

[13] O. M. Magnussen, J. Hotlos, R. J. Nichols, D. M. Kolb, and R. J. Behm, Phys. Rev. Lett. **64**, 2929 (1990).

[14] O. M. Magnussen, J. Hotlos, G. Beitel, D. M. Kolb, and R. J. Behm, J. Vac. Sci. Technol. B **9**, 969 (1991).

[15] J. Clavilier, R. Faure, G. Guinet, and R. Durand, J. Electroanal. Chem. **107**, 205 (1980).

[16] M. Benje, M. Eiermann, U. Pittermann, and K. G. Weil, Ber. Bunsen-Ges. Phys. Chem. **90**, 435 (1986).

[17] M. Zhou, N. Myung, X. Chen, and K. Rajeshwar, J. Electroanal. Chem. **398**, 5 (1995).

[18] F. Möller, J. Kintrup, A. Lachenwitzer, O. M. Magnussen, and R. J. Behm (unpublished).

[19] M. Fleischmann and A. Saraby-Reintjes, Electrochim. Acta **29**, 69 (1984).

[20] C. Wöll, S. Chiang, R. J. Wilson, and P. H. Lippel, Phys. Rev. B **39**, 7988 (1989).

[21] J. V. Barth, H. Brune, G. Ertl, and R. J. Behm, Phys. Rev. B **42**, 9307 (1990).

[22] X. Gao, A. Hamelin, and M. J. Weaver, J. Chem. Phys. **95**, 6993 (1991).

[23] N. J. Tao and S. M. Lindsay, Surf. Sci. **274**, L546 (1992).

[24] J. Wang, B. M. Ocko, A. J. Davenport, and H. S. Isaacs, Phys. Rev. B **46**, 10 321 (1992).

[25] L. P. Nielsen, F. Besenbacher, I. Stensgaard, E. Lægsgaard, C. Engdahl, P. Stoltze, K. W. Jacobsen, and J. K. Norskov, Phys. Rev. Lett. **71**, 754 (1993).